

# Design of bioreactor based on immobilized laccase on silica-chitosan support for phenol removal in continuous mode

A.M. Girelli\*, L.Quattrocchi and F.R. Scuto

Department of Chemistry, Sapienza University of Rome, P.le A. Moro 5, 00185, Rome, Italy

## Abstract

A silica-chitosan support was employed for laccase immobilization. The hybrid support was obtained using calcium ion as linking agent that coordinates silanol and hydroxyl groups of chitosan. The insoluble biocatalyst was then packed in a column and used in a flow system for phenol removal. The immobilized enzyme reactor (IMER) showed a good storage stability (70% of activity in 70 days) and good reusability (90-50% of catalytic activity at the 4th reuse in function of chitosan type). The best performance for the phenol removal was obtained with a low molecular weight chitosan from crab shells at pH 5 and with a flow rate of 0.7 mL/min. The apparent Michaelis–Menten ( $V_{\max}^{\text{app}}$ ,  $K_m^{\text{app}}$ ) and the inherent ( $V_{\max}^{\text{inh}}$ ,  $K_m^{\text{inh}}$ ) constants were also determined to evaluate the influence of the phenol structure on the performance of the system. The enzymatic oxidation of a phenol mixture (4-methylcatechol, catechol, caffeic acid, syringic acid, vanillic acid, p-coumaric acid, and tyrosol) was followed for 21 h in a continuous mode by HPLC. The phenol mixture removal of 90% was also confirmed by Folin-Ciocalteu assay.

**Keywords:** immobilized laccase, continuous mode, silica-chitosan support.

\* Corresponding author: Prof. Anna Maria Girelli

[annamaria.girelli@uniroma1.it](mailto:annamaria.girelli@uniroma1.it)

Tel: (+39) 06 4991 747

## 28 **1.Introduction**

29 The second half of the last century witnessed a rapid deterioration of water environment as a result  
30 of the enormous use of many pollutants, which were conventionally discharged into wastewater  
31 (Papadaki et al., 2004). Phenolic compounds are among the chemicals of greatest concern as they  
32 tend to persist in the environment for a long time, accumulate and exert toxic effects on humans and  
33 animals (Anku et al. 2016) even at low concentrations. In addition they can be transformed into other  
34 fractions more harmful than the original compounds (Vione et al. 2002). A typical example is the  
35 nitration of phenol with nitrite ion on photoinduced oxidation with the formation of 2 - and 4-  
36 nitrophenols. Catechols can be oxidized to semiquinone radicals and at a later stage to o-  
37 benzoquinones when the reaction is catalyzed by heavy metals (Kulkarni & Kaware, 2013). For this  
38 reason, phenolic compounds are included in the list of priority pollutants of the United Environmental  
39 Protection Agency (EPA, 2014) and European Union list 74/464.

40 In particular the phenolic compounds in oil mill wastewater (OMW) are present in concentration  
41 range from 0.5 to 24 mg / LOMW (Rahmanian et al. 2013) and if they are released directly into the  
42 environment without any treatment they can accumulate on the soils causing problems of flora, fauna  
43 and groundwater. Contamination. Typically, phenol concentrations range from 0.5 to 24 mg / LOMW  
44 (Rahmanian et al. 2013). Various techniques for phenol removal have been proposed (Rayati &  
45 Nejabat, 2017; Soni et al. 2017; Yu et al., 2017), such as conventional methods and advanced methods  
46 (AOP). As for conventional treatments there are distillation, adsorption, extraction and chemical  
47 oxidation, which show high efficiencies against various phenolic compounds (Dakhil, 2013).

48 However, conventional processes can have serious shortcomings, such as incomplete removal,  
49 formation of dangerous by-products, low efficiency and applicability at limited concentration ranges  
50 (Villegas et al., 2016; Villalobos & Buchanan, 2002). Due to their weaknesses, current wastewater  
51 treatment technologies are considered ineffective in the complete removal of pollutants, especially  
52 organic matter. For this reason, advanced oxidation processes (AOP) have been developed, which use

53 a combination of oxidizing agents ( $\text{H}_2\text{O}_2$  or  $\text{O}_3$ ), irradiation (UV or ultrasound) and catalysts (metal  
54 ions or photocatalysts) (Kordatou et al., 2018). Obviously, the first indispensable parameter for  
55 choosing the best criterion is the level of abatement of pollutants to be obtained, according to the  
56 precise terms of the law to be respected, both at national and European level. Once it was established  
57 which processes are capable of achieving the objective or not, cost-effectiveness has become the  
58 determining parameter if the efficiency is the same as the chosen methods.

59 However, despite the great efficiency of AOPs, they have numerous disadvantages: relatively high  
60 operating costs due to the use of expensive chemical reagents, increased energy consumption and the  
61 formation of unknown intermediates which in some cases may be more toxic than the starting  
62 compounds (Stasinakis, 2008). Nowadays, the current demand for sustainable methodologies has led  
63 to an increase in the use of oxidoreductases in industrial processes, since their use has numerous  
64 advantages such as biodegradability and catalytic efficiency (Villegas et al., 2016). However, the  
65 harsh industrial conditions cause the enzymes to destabilize, increasing their denaturation. For this  
66 reason, the attachment of enzymes to solid particles gives further rigidity and stability to the three-  
67 dimensional structure of the protein, which is essential for its activity. Furthermore, immobilization  
68 simplifies the management of the biocatalyst and the control of the reaction process, providing easy  
69 separation of the enzyme from the product (Mahat & Onojaq, 2016). The combination of both  
70 attributes facilitates the reuse of the catalyst in various reaction cycles which increases the economy  
71 of industrial biocatalytic processes. Furthermore, the insolubilization of the enzyme confers other  
72 advantages, such as improving the stability of the enzyme against temperature, solvents, pH,  
73 contaminants and impurities, and improving storage stability (Ji et al., 2017; Liu et al., 2012)

74 Nevertheless, the enzyme immobilization may denatured the protein. It is caused by distortions,  
75 especially if some multi-interactions between the enzyme and matrix occur (Tusek et al., 2013).  
76 Nowadays, immobilized enzymes are used for high-fructose corn syrup production, pectin hydrolysis,  
77 fruit juices clarification, interesterification of food fats and oils, biodiesel production (Di Cosimo et

78 al., 2013), and in particular with polyphenol oxidases for detoxification of environmental pollutants,  
79 in the decolorization of textile wastewater and in the treatment of pulp and paper (Guzik et al., 2014).  
80 As well known, white rot basidiomycetes are the most efficient lignin degraders by means of  
81 oxidative reactions catalyzed by phenol oxidases and peroxidases. Between them laccase, a multi-  
82 copper enzyme, shows good efficiency in the phenol removal (Tusek et al., 2013; Liu et al., 2012)  
83 and in particular *Trametes versicolor* appeared to be one of the best pollutant degrader by reducing  
84 phenol by up to 88 % (Rahmanian et al. 2013).

85 In this scenario, the aim of this study was to point out an insolubilization system of laccase from  
86 *Trametes versicolor* by immobilization on a new support, as silica-chitosan, for the removal of  
87 various phenols selected among those most present in the OMW from water: phenolic acids (caffeic,  
88 p-coumaric, syringic, vanillic), alcoholics (tyrosol) and classic (catechol and 4-methylcatechol).  
89 Many studies have previously dealt with immobilized laccase on microparticles, as for examples, of  
90 silica beads (Rahmani et al., 2015; Champagne & Ramsay, 2007) and of chitosan beads (Apriceno et  
91 al., 2019; Zheng et al., 2016) and on nanoparticles of silica-coated magnetic nanoparticles  
92 ( $\text{Fe}_3\text{O}_4@SiO_2$ ) (Moldes-Diz et al. , 2018) and of zirconia-silica hybrid support (Jankowska et al.  
93 2019) but it has not been never employed a hybrid support of silica and chitosan. In particular, the  
94 linear biopolymer is composed of randomly distributed  $\beta$ -(1-4) linked D-glucosamine (deacetylated  
95 unit) and N-acetyl-D glucosamine (acetylated unit) having several hydroxyls and a number of reactive  
96 amine groups in function of deacetylated degree. Therefore, the preparation of the hybrid support  
97 was obtained adsorbing Ca (II) ions on chitosan and silica by chelation through OH or  $\text{NH}_2$  groups  
98 of biopolymer and silanol groups. (Carunchio et al., 1987). In this way it is possible to exploit the  
99 good thermal and chemical stability, as well as excellent mechanical resistance and high surface area  
100 of silica with the biodegradability, biocompatibility, non-toxicity, inexpensiveness, as well as the  
101 good ability to bind the enzymes, of chitosan (Girelli et al., 2020). In addition, with the aim of  
102 preserving the catalytic activity of the enzyme, the glycosidic part of the enzyme was involved in the  
103 immobilization procedure (Girelli et al., 2020). This peculiarity was obtained treating laccase with

104 periodate in order to oxidize hydroxyl to aldehydic groups, highly reactive with the available amino  
105 groups of chitosan, through the formation of a covalent imine bond type (Apriceno et al., 2018). The  
106 whole immobilization process is illustrated in figure 1.

107 The biocatalyst was then employed in a laboratory-scale reactor in order to be used in a continuous  
108 mode. The optimization of key parameters such as type of chitosan and hydrodynamic parameter  
109 (flow rate) were investigated. In addition, kinetic parameters, storage and operative stability of  
110 bioreactor were performed. The enzymatic oxidation of single phenol and of a model mixture was  
111 made in a continuous mode. IMER results were compared of enzymatic with those obtained by the  
112 Folin-Ciocalteu spectrophotometric method (Lamuela-Raventos, 2018).

113

## 114 **2. Materials and methods**

### 115 *2.1. Chemical and reagents*

116 Laccase from *Trametes versicolor* with a nominal activity of 136 U/mg protein, 2,2-azinobis (3-  
117 ethylbenzothiazoline-6-sulfonicacid)diammonium salt (ABTS), chitosan from crab shells with low  
118 molecular weight (50-190 KDa) (CS1), chitosan from crab shells with medium molecular weight  
119 (CS2) (~400 KDa) and chitosan from shrimp shells (CS3) were purchased from Sigma-Aldrich.  
120 Potassium meta-periodate was purchased from Carlo Erba (Milan, Italy). Silica LichrosorbSi 60  
121 (5 $\mu$ m)(Merck). Caffeic acid ( $\geq 98\%$ ), catechol ( $\geq 99\%$ ), p-coumaric acid ( $\geq 98\%$ ), 4-methylcatechol  
122 ( $\geq 95\%$ ), siringic acid ( $\geq 95\%$ ), tyrosol and vanillic acid ( $\geq 97\%$ ) were purchased from Sigma-Aldrich.

### 123 *2.2. Chitosan characterization*

124 The chitosan characterization was performed by elemental analysis, using the analyzer EA 1110  
125 CHNS-O. The degree of deacetylation (DD%) was calculated, in accordance to Kaasai,2000, from  
126 the carbon/nitrogen (C/N) ratio as follows:

127  $DD\% = 100 - ((C/N - 5.145) / (6.861 - 5.145)) * 100$

128 C/N is carbon/nitrogen ratio that varies from 5.145 in completely N-deacetylated chitosan to 6.816 in  
129 chitin, the fully N-acetylated polymer.

### 130 *2.3 Preparation of silica-chitosan support*

131 1 g of silica was placed under stirring in 40 mL of a 0.05 M  $\text{Ca}(\text{NO}_3)_2$  solution at pH 7 for 30 min at  
132 room temperature. Then, it was filtered with a 3 D4 gooch and washed with distilled water until the  
133 excess of calcium was removed.

134 Contemporary, in order to dissolve chitosan and obtain a homogenous solution, 0.45 g of chitosan  
135 (CS) were placed in 30 mL 1% acetic acid solution under stirring. Successively, pretreated silica was  
136 added to 12 mL of CS solution and brought volume to 20 mL with deionized water. After 3 hours,  
137 the aqueous phase was removed by evaporation under vacuum. The solid phase was finally washed  
138 in turn with a methanolic solution of potassium hydroxide 0.1 M, methanol and distilled water.

### 139 *2.4 Laccase immobilization procedure*

140 150 mg silica-chitosan support were incubated with 1 mL of oxidized laccase (0.4 U) at pH 7 for 24  
141 h. Then the biocatalyst was washed with deionized water and stored at 4°C. The oxidized laccase was  
142 obtained by periodate oxidation, as previously reported, by the authors (Apriceno et al., 2018).

143 For the flow system, a stainless-steel column ( 5 cm x 2.1 mm) was dry-packed with ~ 60 mg of  
144 biocatalyst and connected between the HPLC pump and the UV-vis detector. The system was  
145 equilibrated with 0.1 M citrate-0.2 M phosphate buffer pH 5 for 15 min before use. The IMER was  
146 stored when not in use at 4°C after washing treatment with deionized water

### 147 *2.5 Enzymatic activity assay*

148 Procedure in batch system: 2mL of 0.23 mM ABTS were added to 10 mg/10 $\mu$ L of immobilized/free  
149 laccase in a 0.1 M citrate-0.2 M phosphate buffer solution (pH 3.0) until to reach a final volume of  
150 2.7 mL. The laccase activity was detected at 30°C following the enzymatic formation of radical cation

151 ABTS<sup>+</sup> at 420 nm. In this way one unit of enzymatic activity was defined as the amount of enzyme  
152 required to oxidize 1 μmol of ABTS per minute.

153 Procedure in the flow system: 20 μL of 2.5 mM ABTS solution were injected onto the HPLC system  
154 (composed by the pump, the IMER as stationary phase and the UV-vis detector) and employing a 0.1  
155 M citrate-0.2 M phosphate buffer at pH 5 as eluent. The amount of ABTS radical cation (ABTS<sup>+</sup>)  
156 formed, detected at 420 nm, was pursued by integration of peak areas and by interpolation with a  
157 calibration curve previously obtained. Since ABTS cation radical was not available in commerce, it  
158 was generated by chemical oxidation of ABTS by sodium persulfate, as reported by Re et al., 1999.  
159 Thus, 8 mL of 0.093 mM ABTS and 2 mL of 12.5 mM sodium persulfate was kept in a flask in the  
160 dark and at room temperature for 16 hours in order to obtain a stable product. The amount of ABTS  
161 radical cation (ABTS<sup>+</sup>) was detected at 420 nm by a UV-vis spectrophotometer (PG Instrument  
162 Limited, Leicester, United Kingdom), considering its molar extinction coefficient ( $\epsilon = 36000$   
163 mol/L\*cm). Successively, the solution was diluted several times obtaining a series of standard  
164 solutions. Then, 20 μL of each diluted standard solution were directly injected in HPLC system, using  
165 silica-chitosan support, without immobilized enzyme, as stationary phase and 0.1 M citrate/0.2 M  
166 phosphate buffer pH 5 as eluent. A calibration curve was obtained reporting the ABTS<sup>+</sup> peak areas,  
167 at 420 nm, in the range 0.0005-0.004 μmol of ABTS radical ( $y=1.04 \cdot 10^7x - 1.06 \cdot 10^3$  ;  $r^2 = 0.994$ ) .

## 168 *2.6 Immobilization Parameters*

169 The immobilization yield, efficiency and recovery were calculated by the following formulas:

$$170 \quad \text{Immobilization yield (IY)(\%)} = 100 \times ((U_0 - U_f) / U_0) \quad (1)$$

$$171 \quad \text{Efficiency (E)(\%)} = 100 \times U_s / (U_0 - U_f) \quad (2)$$

$$172 \quad \text{Recovery (R)(\%)} = 100 \times U_s / U_0 \quad (3)$$

173 where  $U_0$  and  $U_f$  are laccase activity in the solution before and after the immobilization process,  
174 respectively, while  $U_s$  is the activity of the immobilized laccase.

175

### 176 *2.7 Effect of chitosan types*

177 The effect of 3 chitosan types (CS1, CS2 and CS3) with different molecular weight on the biocatalyst  
178 performance was evaluated in “batch” system by comparing the operative stability and the  
179 immobilization parameters (immobilization yield, efficiency and recovery) of the biocatalyst.

### 180 *2.8 Effect of flow rate on IMER performance*

181 A fixed ABTS amount (0.25 mM) was injected onto the HPLC system: the stationary phase was the  
182 thermostated IMER at 30°C, and the mobile phase was 0.1 M citrate-0.2 M phosphate buffer pH 5.  
183 The injections were made in triplicate at different flow rates (0.5-0.8 mL/min)

### 184 *2.9 Determination of operational stability*

185 Procedure in batch system: The operational stability of the biocatalysts was assessed in successive  
186 batch reaction cycles. After every cycle the system was washed three times with 0.1 M citrate-0.2 M  
187 phosphate buffer and was refilled with fresh ABTS substrate in order to detecting the activity of the  
188 biocatalyst. The relative enzymatic activity of each cycle was referred to the activity of the first use.

189 Procedure in flow system: The operative stability of IMER was evaluated detecting the activity in 4  
190 cycles and taking in consideration the ABTS injections in every cycle. The IMER activity was  
191 detected injecting 20  $\mu$ L of a fresh substrate solution (2.5 mM) in 0.1 M citrate-0.2 M phosphate  
192 buffer pH 5. Finally, the IMER was regenerated with deionized water as mobile phase in order to  
193 remove any traces of substrates and products. Then IMER was reused for a new cycle of injections  
194 under the same conditions. The relative enzymatic activity of each cycle was referred to the activity  
195 of the initial activity (first cycle).



196 *2.10 Determination of storage stability*

197 The storage stability of IMER and free laccase was assessed by activity evaluation over a 70-day  
198 period. The IMER and free laccase were maintained at 4 °C when not in use. The activity assay of  
199 both enzymatic forms was carried out as above described.

200 *2.11 Determination of phenol kinetic parameters*

201 In order to verify the laccase action on all the phenols, a UV-visible spectroscopic study was,  
202 previously, performed. For this reason, 10 mg of each phenol were dissolved in the minimum amount  
203 of ethanol and brought at volume to 10 mL with deionized water. Then a preliminary investigation  
204 on each phenol oxidation by laccase was performed in order to individuate the enzymatic reaction  
205 and the operative wavelengths. For this reason, 10 µL of free laccase solution (3 U) were added to 2  
206 mL of diluted phenol 1:10 (v/v). The UV- spectra were successively recorded every 10 min for one  
207 hour. At the end of the analysis, it appeared that tyrosol and p-coumaric acid were not oxidized by  
208 the enzyme while the catechol and 4-methyl-catechol showed a product at 400 nm, the syringic acid  
209 at 360 nm, the caffeic acid at 412 nm and the vanillic acid at 390 nm.

210 For the determination of kinetic parameters, the IMER at 30°C, was firstly equilibrated for 15 min  
211 with 0.1 M citrate-0.2 M phosphate buffer pH 5. Then, 20 µL of each phenol solution (caffeic acid,  
212 catechol, p-coumaric acid, 4-methylcatechol, syringic acid, tyrosol and vanillic acid), were injected  
213 into the HPLC with a flow rate of 0.7 mL/min of 0.1 M citrate-0.2 M phosphate buffer pH 5, as  
214 mobile phase. The quinones enzymatically formed were chromatographically detected at the  
215 respective maxima wavelengths. The Michaelis-Menten curve was obtained reporting the reaction  
216 rates, expressed as the ratio of the products peak areas on the retention times (area/min) as a function  
217 of the concentration of injected phenol. The kinetic parameters were determined by the Lineaweaver-  
218 Burk method. The inherent kinetic parameters were, instead, calculated with the Engasser-Horvath  
219 graphic method (Engasser-Horvath, 1976).

220 *2.12 Phenolic compounds bioremediation*

221 For the phenol removal investigations, the stainless-steel column filled with the immobilized laccase  
222 was thermostated at 30°C. 10 mL of a solution containing 75 mg/L of phenol in 0.1 M citrate-0.2 M  
223 phosphate buffer pH 5 were pumped and recycled through the IMER at 0.7 mL/min. The degradation  
224 was followed both with the spectrophotometric method of Folin-Ciocalteu, for the determination of  
225 total phenol content, and with the HPLC method, to evaluate the kinetic of each individual phenol.  
226 For both methods, aliquots of sample were taken at set time intervals (8, 14, 21 h) without interrupting  
227 the continuous flow system.

228 With the HPLC the unremoved phenol amount was chromatographically detected at 280 nm. 20 µL  
229 of aliquots drawn from reservoir with a flow rate of 0.7 mL/min were injected in a HPLC system at  
230 fixed time. The elution was performed employing a gradient between pump A: MeOH: H<sub>2</sub>O with  
231 1.3% HCOOH and pump B: deionized H<sub>2</sub>O. The optimized gradient was: 0 to 24 min 15% of A, 24  
232 to 35 min 50% A, 35 to 38 min 50% A and 38 to 40 min 20% A. The stationary phase was a prosphere  
233 reversed phase C18 column (5 µm) (15 cm x 4.6 mm ID) (Sigma-Aldrich).

234 For the spectrophotometric Folin-Ciocalteu (FC) method (Lamuela-Raventos, 2018) aliquots of 0.1  
235 mL drawn from reservoir of the phenol mixture was prelevated and put in a 10 mL volume flask.  
236 Then 5 mL of deionized water, 0.5 mL of FC reagent, 2 mL of a 20% (w/v) sodium carbonate solution  
237 (Na<sub>2</sub>CO<sub>3</sub>) and deionized water until to reach 10 mL were added. The sample was kept for 30 min at  
238 40 °C and the absorbance was subsequently read at a wavelength of 760 nm against a blank prepared  
239 under the same conditions of the sample but replacing the phenols with the citrate phosphate buffer  
240 at pH 5. The total phenol concentration, expressed as equivalents (mg/L) of gallic acid, was  
241 determined with a calibration curve obtained by appropriately diluting a solution of gallic acid,  
242 prepared by dissolving 0.5 g of gallic acid in 10 mL of ethanol and brought to volume in a 100 mL  
243 flask with deionized water. The analysis was then performed in the same way as the samples.

### 244 **3. Results and discussion**

245 The study was initially focalized on the characterization of the hybrid support aimed both for  
246 confirming the composite formation and to choose the chitosan with the highest number of amine  
247 groups available for immine bonds with the CHO groups of oxidized laccase. Thus, the evaluation  
248 was made on the basis of deacetylation degree and the amount of chitosan adsorbed on silica. For the  
249 continuous mode it was also fundamental considering the IMER back pressure.

### 250 *3.1 Chitosan and chitosan-silica support characterization*

251 Generally, the methods used to determine the chitosan deacetylation degree are spectroscopic (IR and  
252 NMR), conventional (titration, conductivity, potentiometry) and destructive (elemental analysis and  
253 hydrolysis). The elemental analysis has the advantage of being able to be used in the whole range of  
254 deacetylation degree in comparison to the other techniques (Kaasai, 2009). The values obtained on  
255 the basis of elemental analysis, for the different chitosan samples (table 1), are 78.8%, 74.4% and  
256 70.4 % for CS1, CS2 and CS3, respectively. It appears that chitosan with low molecular weight (CS1)  
257 shows the highest degree of deacetylation and the highest percentage of amino groups that can then  
258 be involved in the covalent bond with the enzyme. Furthermore, taking into account that % C depends  
259 on the molecular weight (PM) of chitosan it is predictable that CS3 has the highest molecular weight  
260 having the highest % C.

261 The elemental analysis of the composites was also carried out in order to verify the chitosan coating  
262 in the various composites (table 1). Nitrogen is present exclusively in chitosan and comparing its  
263 percentages in the different composites with those in the respective chitosan type, it is predictable a  
264 25%, 17% and 14% of silica covering CS3, CS1, and CS2, respectively.

265 The investigation was also evaluated by thermogravimetric analysis (TGA). In figure 2 the thermo  
266 analytical behavior of silica, pure chitosan and 3 composites of silica-chitosan in the temperatures  
267 range between 0 to 700 °C are reported. It appears that chitosan alone shows a weight loss that starts  
268 at 270 °C, which is unseen in silica curve. The weight loss indicates that chitosan is starting to  
269 decompose at this temperature until to reach a plateau of 30% of its initial weight at approximately

270 700°C. Similar thermogravimetric curves are achieved with the composites but different percentages  
271 of weight loss are obtained. On the basis of the residual weights it is possible to determine the  
272 following degree of silica coverage by chitosan: 20% for CS3, 16% for CS1 and 14% for CS2. The  
273 reached results are in good accordance with those of elemental analysis.

### 274 3.2 Choice of chitosan

275 To evaluate the type of chitosan (CS1, CS2, CS3) for attaining the best performance of the  
276 biocatalysts: operational stability, immobilization parameters (efficiency, recovery and immobilized  
277 activity), and the counter-pressures generated by the supports silica-CS in the flow system were  
278 investigated.

279 The operative stability is a very important parameter in the industrial field, since it allows the reuse  
280 of the enzyme and the reduction of the process costs. Repetitive measurements of the 3 biocatalysts  
281 activity were carried out in "batch" system. The immobilized activity % of each biocatalyst,  
282 employing ABTS as substrate, is shown in figure 3. From the histograms it appears that the biocatalyst  
283 with silica-CS3 presents the highest operative stability since at the ninth recycle it retains an activity  
284 of ~80%, while those with silica-CS1 and silica-CS2 only 50% and 35%, respectively. In addition,  
285 since the optimized method must be used in a continuous flow system where back pressures have a  
286 fundamental role to allow the analysis, 3 columns were filled with 60 mg of silica-CS1/CS2/CS3  
287 supports and connected to an HPLC pump. The back pressures of the different supports using water  
288 as eluent were determined. Results showed that chitosan from shrimp shells (CS3) had the highest  
289 counter-pressure value (>250 bar), CS2 27 bar and CS1 the best value (0 bar). This behavior was  
290 directly correlated to the chitosan molecular weight ( $MW_{CS1} = 50-190$  KDa,  $MW_{CS2} = 400$  KDa) and  
291 viscosity (CS1= 20-300 cP, CS2 >400 cP). CS3, which is presumed to have the greatest molecular  
292 weight and viscosity, may increase the resistance to the passage of the eluent phase.

293 In conclusion, it can be established that "shrimp shells" chitosan (CS3) turns out to be the best for a  
294 possible use in "batch" system, since maintains the greatest activity in reuse tests but in a continuous

295 flow system, the choice of chitosan must be made between CS1 and CS2 which have generated lower  
296 back pressure. By the immobilization parameters comparison appears that activity yield (92%),  
297 efficiency (32%) and recovery (29%) values are 92%, 32% and 29% for CSI while 86%, 9%, 8% for  
298 CS2, respectively. These different values are due to the highest deacetylation degree (78.8%) and  
299 chitosan amount adsorbed on silica (17%) for CS1. Finally, considering also the operative stability  
300 the choice was focused on chitosan from crab shells with low PM (CS1).

### 301 *3.3. Optimization of the parameters influencing the phenol removal*

302 The choice of chitosan and the optimization of different parameters like pH, temperature, flow rate  
303 for the phenol removal in the continuous flow reactor (IMER) were investigated. In the figure 4 the  
304 recycle device used for phenol removal is reported.

#### 305 *3.3.1 Choice of pH*

306 The choice of the most suitable pH was carried out on silica-CS1 system. Considering the data  
307 previously reported by the same authors (Girelli et al., 2020) where the results evidenced the highest  
308 activity at pH 3 and an high pH tolerance until pH 5.5 towards ABTS and that pH 5 is the value very  
309 close to OMW samples (Mulinacci et al., 2001), pH 3 and pH 5 were chosen. In addition, taking into  
310 account that biocatalyst application was in continuous mode, the study was made fluxing citrate  
311 phosphate buffers on IMER. A back pressure of 110 psi at pH 3 appeared since it may be due to  
312 chitosan swelling that increases with pH decreasing. (Rohindra et al., 2004). At pH 5 a low back  
313 pressure was instead obtained (<10 psi) indicating a more favorable pH condition for the employment  
314 of IMER in continuous mode. This result together with the slight lower laccase activity at pH 5 than  
315 pH 3 (Girelli et al. 2020), the value of 5 was chosen as the operating pH.

#### 316 *3.3.2. Choice of hydrodynamic parameter*

317 The flow rate of the mobile phase, which is a key parameter in a continuous reaction was also  
318 investigated. This parameter influences the residence time of the reagents in the IMER, the diffusion

319 rate of the substrate towards the active site and of the product towards the mobile phase. Since the  
320 mass transfer limitations arising from immobilization is manifested in an increase in the apparent  
321 values of the Michaelis-Menten constants, a study on the individuation of the kinetic parameters at  
322 different flow rates was performed. For this reason, different amount of ABTS in the range 0-3.82  
323 mM at pH 5 and 30°C were injected into the chromatographic system in order to determine the rate  
324 of ABTS radical cation formation. The apparent values of  $K_m^{app}$  and  $V_{max}^{app}$  were estimated by the  
325 double reciprocal plots of  $1/v$  versus  $1/[ABTS]$ . From the results reported in table 2 it is observed that  
326 as the flow rate increases from 0.5 to 0.7 mL/min the  $K_m^{app}$  values tend to decrease, while above 0.7  
327 mL/min it tends to slightly increase. This behavior should be due to the fact that the flow rate  
328 influences the contact time between the enzyme- substrate (figure S1) and the diffusion of the  
329 substrate and product towards the active sites and mobile phase, respectively. For low flow values (<  
330 0.7 mL/min) the predominant effect is the diffusion resistance, while for high flow (> 0.7 mL/min)  
331 the contact time becomes short and the efficiency activity tends to decrease.

332 To eliminate the effect of external diffusion, the inherent kinetic parameters ( $K_m^{inh}$ ,  $V_{max}^{inh}$ ) were  
333 determined by Engasser-Horvath graphical method (Engasser & Horvath, 1976). In this way,  
334 assuming that substrate was consumed on the enzyme surface, the laccase activity and the kinetic  
335 parameters in the absence of diffusion limitations were evaluated. In order to evaluate it is, however,  
336 necessary to consider the surface area present inside the bioreactor (obtained by the product of silica  
337 specific surface area (500m<sup>2</sup>/g) with the amount of support) and to normalize the amount of formed  
338 product respect the retention time and the surface area. The determination of the inherent kinetic  
339 parameters is obtained starting from the Michaelis-Menten experimental curve, and tracing to it the  
340 tangent at the point of origin, in order to determine the mass transport coefficient "h" as reported by  
341 Girelli et al., 2007. Subsequently, it was possible to determine the ABTS amount on the external  
342 biocatalyst surface at the different rates in order to obtain a new Michaelis-Menten curve. The  
343  $K_m^{app}$ ,  $V_{max}^{app}$  parameters and the mass transport coefficients "h" are shown in table 2 in function of  
344 flow rates. It appears that  $K_m^{inh}$  values decrease with increasing flow rates until 0.8 mL/min while the

345 parameter "h" tends to increase until 0.7 mL/min and above this value tends to decrease. Therefore  
346 0.7 mL/min was chosen as optimal flow rate.

#### 347 *3.4. IMER repeatability*

348 In order to assess the reliability of the immobilization process, two equal IMERs, obtained packing  
349 two columns (5 cm x 2.1 mm) with silica-chitosan-laccase, were tested. In this way it was possible  
350 to compare the activity measured of both IMERs, injecting 20  $\mu$ L of a 2.5 mM ABTS solution into  
351 chromatographic system composed by the pump, IMER and UV detector. The mean peak area values  
352 of the radical product enzymatically formed for IMER1 and IMER2 were 46859 and 54535,  
353 respectively. The variation coefficient (CV%) of 7.5 % highlighted that the repeatability of the  
354 bioreactors preparation was good.

355 As regards the repeatability of IMER intra-day response the investigation was performed injecting  
356 for 5 times 20  $\mu$ L of a 2.5 mM ABTS solution into the HPLC system. A CV value of 1.7 % showed  
357 a good repeatability of the measurements.

#### 358 *3.5. Operational and storage stability of IMER*

359 Operational and storage stability of IMER with laccase immobilized on silica-CS1 support were  
360 investigated. since industrial applications require costs reduction. In both cases, the laccase  
361 immobilized activity was determined in continuous mode through the analysis of ABTS product peak  
362 areas.

363 For the IMER storage stability at 4°C (when not in use), the measurements after 30, 50 and 70 days  
364 were performed. Results, shown in fig 5a, evidence at 70 days a IMER residual activity value of 70%  
365 and only 15% for free laccase. This result is very promising since it is possible to store laccase in a  
366 more suitable form and ready to use than the soluble form. This finding can be due to the laccase  
367 binding on the support that avoid molecules aggregation and alterations in protein conformation.

368 The reuse of IMER in a continuous mode was assessed according to the number of ABTS injection  
369 in the flow system and measuring the activity of the IMER at the starting analysis (cycle 1), after 50

370 injections (cycle 2), 80 injections (cycle 3) and 105 injections (cycle 4). From figure 5b it is possible  
371 to evidence that after 50 injections (cycle 2) the activity decreases of 30% which remains almost  
372 constant for 80 injections (cycle 3). In the fourth cycle (after 105 injections) the residual activity tends  
373 to decrease slowly until 50% value. However, the decrease in the activity of the immobilized laccase  
374 as a result of repeated uses was expected due to the possibility of enzyme denaturation and release  
375 during the operation process.

376 In table 3 the performance and the storage stability of laccase immobilized on various supports,  
377 recently published in literature, are compared with those of the proposed biocatalyst. In particular  
378 from the table, it appears the biocatalyst obtained in the present study is the only one applied in a  
379 continuous mode which is easier and cheaper technology than the batch mode. In addition the system  
380 also highlights a storage and operative stability comparable to those of other biocatalysts.

### 381 *3.6. Kinetic parameters of phenol compounds*

382 Once the phenol affinity for free laccase was verified, the apparent and inherent kinetic parameters  
383 of each phenol in the continuous system were determined in order to individuate the affinity of each  
384 phenol with laccase. As, well known the activity efficiency of an oxidoreductase as laccase, is  
385 correlated to electron transfer from the substrate to the T1 Cu and the difference ( $\Delta E_p$ ) between the  
386 redox potentials of the substrate and the T1 Cu is the main driving force for the reaction, together  
387 with the substrate binding affinity (Xiu et al., 2001). In literature (Gonzalez et al., 2009; Gianfreda et  
388 al., 1999) the laccase affinity influence on chemical phenol structure is also reported. Gianfreda et  
389 al., 1999, reported the effect of the number and position of hydroxyl groups on the aromatic ring, the  
390 nature and molecular mass of the substituents. Gonzalez et al., 2009, evidenced that the substrate  
391 affinity towards laccase varies with the substituent position on the aromatic ring (para > meta > ortho).  
392 Results obtained in this study show that for the apparent kinetic parameters, reported in table 4,  
393 syringic acid has the greatest affinity for active sites of laccase immobilized, followed by caffeic acid,  
394 vanillic acid, 4-methylcatechol, and finally catechol while tyrosol and p-coumaric acid presented no



395 reactivity towards laccase. However, the order obtained in this study does not agree with the  
396 electrochemical properties of the compounds, probably due to different external and internal diffusion  
397 and partition effects of phenol with the immobilized enzyme (Goldstein, 1976). It appeared, that the  
398 biocatalyst performance depends strictly by the presence of the carboxylic acid group in the phenolic  
399 structure. In fact, syringic, vanillic, and caffeic acid at pH 5 has a negative charge for the  
400 deprotonation of COOH group (pKa 3.1-4.2), as shown in table 5, and their diffusion toward active  
401 sites of enzyme can be favored for an attractive force of the free protonated amino groups residue of  
402 chitosan (pKa 6.5) (Wang et al., 2006) and/or of the protein (pKa 6) (Scheiblbrandner et al., 2017).  
403 For simple phenols and tyrosol it appeared that the hydrophobicity, expressed by logP, was the crucial  
404 parameter that influenced the apparent kinetic parameters values (table 5). This is confirmed by the  
405 fact that catechol and tyrosol with the lowest logP had the lowest enzymatic reaction rate.  
406 So, it is possible to confirm that the kinetic parameters are affected by a number of factors, including  
407 redox potential and diffusive and electrostatic phenomena which alter the concentration of substrates  
408 at the laccase active sites from bulk solution values.

409 In order to obtain the kinetic parameters of the individual phenol in absence of the diffusional effects,  
410 the inherent constants were determined following the Engasser–Horvath method (Engasser–Horvath,  
411 1976). The results, reported in table 4, evidence that  $K_m^{inh}$  values, especially for catechol and 4-  
412 methylcatechol, are lower than the correspondent  $K_m^{app}$  and that the phenolic affinity order changes.  
413 The new order shows that 4-methylcatechol (MC) has the highest efficiency activity towards laccase  
414 while caffeic acid the lowest one. This is probably due to the strictly dependence of the chemical  
415 features of the phenolic substrate such as the number of -OH groups present, the nature and molecular  
416 mass of the substituents and their position on the aromatic rings (table 5). In particular 4-  
417 methylcatechol presenting a substituent electron –donating (-CH<sub>3</sub>) easier gives up an electron and  
418 provides an area of greater density in the aromatic ring from which an electron can easily be removed.  
419 This leads to lower oxidation potentials and higher oxidation rate. This is also confirmed by the fact  
420 that catechol respect 4-methylcatechol shows always a very lower enzymatic affinity. By contrast,

421 caffeic acid which has a substituent with electron withdrawing (-COOH) harder gives up an electron  
422 and consequently the increased oxidation potential favors a decreased oxidation rate.

423 However, for the acid phenols it is very difficult to explain the sequence since the activity efficiency  
424 depends also on the architecture of the laccase's substrate-binding pockets, related to the substrate's  
425 steric hindrance and/or on the partitioning effects related to hydrophobic/hydrophilic interaction  
426 (Glazunova et al., 2018; Pardo & Camarero, 2015; Frascioni et al., 2010).

### 427 *3.7. Phenol compounds removal*

428 The removal of phenol in continuous mode, was performed, at 30°C, by recirculating a model of  
429 phenolic mixture solution through IMER and sampling for FC method and for HPLC analysis at  
430 prefixed times. The mixture, constituted by catechol, 4-methylcatechol, tyrosol, vanillic acid, syringic  
431 acid, caffeic acid and p-coumaric acid, at the same mass amount (mg/L) corresponding at different  
432 molar concentration, with the time evidence a change in color from colorless to yellow-pink,  
433 indicating a visible proof of the oxidative reaction (Gianfreda et al., 2003).

434 The effect of phenol concentration on laccase catalytic action was investigated employing three high  
435 total concentration of 175, 350 and 525 mg/L in order to assess the ability of the enzyme to transform  
436 large amount of phenolic compounds. This study was performed spectrophotometrically by FC assay  
437 measuring the total phenolic content, expressed as gallic acid equivalents (mg/L), at fixed times (8  
438 and 14 h). The % degradation, obtained by the %ratio of the residual total phenol amount to the initial  
439 one, increased with the increasing of concentrations from 175 to 350 m/ L and then remained  
440 approximately constant up to 525 mg/L (table 6). This is probably due to the fact that the system  
441 reaches a maximum operating capacity and that a further concentration increase does not lead to any  
442 improvement. In addition, in order to establish the operative degradation time, the mixture at 525  
443 mg/L removal was followed up to 21 h and as result a ~90% % degradation value was obtained. Then,  
444 in order to confirm that the oxidation action was exclusively due to the laccase and not to a natural  
445 degradation process of the phenols, the total phenolic amount was evaluated after a recirculation

446 process employing a reactor filled with only silica-CS1 support. Spectrophotometric results showed  
447 that the absence of any degradation as the amount of 525 mgL<sup>-1</sup> total phenolic compounds,  
448 correspondent to 446 mg/L as gallic acid, remained almost constant (443.6 mg/L of gallic acid) up to  
449 21 h.

450 Then, in order to follow the trend of the oxidation kinetics of individual phenolic compounds by  
451 IMER, the chromatographic analyses were performed at the optimized conditions: 21h as degradation  
452 time and 525 mg/L as amount of total compounds. In figure 6 the chromatograms of phenol removal  
453 after their recirculation through IMER at 0, 14 and 21 h are reported. It is possible to observe the peak  
454 areas decrease of each compound and the formation of further chromatographic peaks, related to  
455 oxidation products.

456 The results have shown that 4-methylcatecol and caffeic acid are the ones that react faster, while the  
457 others start to degrade only after 8 hours (figure 7). It appears that all phenols are almost completely  
458 oxidized by IMER at 21 h (90%).

459 The removal order can be linked to the competitive effects between phenols in the interactions with  
460 the enzyme and to their different molar concentrations (Frasconi et al., 2010). In particular p-coumaric  
461 acid and tyrosol, which alone have a very low reactivity towards laccase, when incubated with the  
462 other phenols, are removed.

463 A further study is hoped to better clarify the process and improve the removal efficiency of the  
464 enzyme.

#### 465 **4. Conclusion**

466 In this work a new immobilization procedure, based on binding of periodate-oxidized laccase onto a  
467 silica-chitosan support through the action of calcium ions which coordinate silanol and hydroxyl  
468 groups of chitosan, is employed for the bioremediation of 7 phenol compounds in water by a  
469 continuous process. The enzymatic activity of the IMER presented good repeatability values and  
470 retained 70% value for 70 days and 50% after more than 105 injections. It also appeared that when

471 all phenols are together, a general increase of the phenol removal was obtained respect than when  
472 they were alone. In particular tyrosol and vanillic acid, that have a very low reactivity towards laccase,  
473 were removed only in the presence of the other phenols. This result is probably due to a “laccase  
474 mediator system” effect ruled by phenols efficiency activity and molar concentrations.

#### 475 **Declaration of competing interest**

476 The authors declare that they have no known competing financial interests or personal relationships  
477 that could have appeared to influence the work reported in this paper.

#### 478 **Acknowledgements**

479 The authors are grateful to the support from University Sapienza of Rome, Italy.

480

#### 481 **Supplementary materials**

482 Supplementary data to this article can be found

483

#### 484 **References**

485 Anku, W.W, Messai, M.A., Govender, P.P. 2016. Phenolic Compounds in Water: Sources,  
486 Reactivity, Toxicity and Treatment Methods. Chapter in a book: Natural Sources, Importance and  
487 Applications <https://doi.org/10.5772/66927>

488 Apriceno, A., Astolfi, M.L., Girelli., A.M., Scuto, F.R., 2019. A new laccase-mediator system facing  
489 the biodegradation challenge: insight into the NSAIDs removal. *Chemosphere* 215, 535-  
490 542. <https://doi.org/10.1016/j.chemosphere.2018.10.086>

491 Apriceno, A., Bucci, R., Girelli, A.M., 2017. Immobilization of laccase from *Trametes versicolor* on  
492 chitosan macrobeads for anthracene degradation. *Anal. Lett.* 50, 2308-  
493 2322. <https://doi.org/10.1080/00032719.2017.1282504>

494 Apriceno, A., Girelli A.M., Scuto, F.R., 2018. Design of a heterogeneous enzymatic catalyst on  
495 chitosan: investigation of the role of conjugation chemistry in the catalytic activity of a Laccase from  
496 *Trametes versicolor*. *J. Chem. Technol. Biotechnol.* 93, 1413-  
497 1420. <https://doi.org/10.1002/jctb.5509>.

498 Canfora, L., Iamarino, G., Rao, M.A., Gianfreda, L., 2008. Oxidative transformation of natural and  
499 synthetic phenolic mixtures by *Trametes versicolor* laccase. *J. Agric. Food Chem.* 56, 1398-  
500 1407. <https://doi.org/10.1021/jf0728350>

501 Carunchio, V., Girelli, A. M., Messina, A., Sinibaldi, M., 1987. Chitosan-coated silica gel as a new  
502 support in high-performance liquid chromatography. *Chromatographia*. 23, 731–  
503 735. <https://doi.org/10.1007/BF02312665>

504 Champagne, P., Ramsay, J., 2007. Reactive blue 19 decolouration by laccase immobilized on silica  
505 beads. *Appl. Microbiol. Biotechnol.* 77, 819–823. <https://doi.org/10.1007/s00253-007-1208-1>

506 Dakhil, I.H., 2013. Removal of phenol from industrial wastewater, using sawdust. *Res. Inventy: Int.*  
507 *J. Eng. Sci.* 3, 25-31.

508 Di Cosimo, R., Mc Auliffe, J., Poulouse, A. J., Bohlmann, G., 2013. Industrial use of immobilized  
509 enzymes. *Chem. Soc. Rev.* 42, 6437. <https://doi.org/10.1039/C3CS35506C>

510 DIRECTIVE 76/464/EEC achievements and obstacles in the implementation of council directive.  
511 76/464/EEC on aquatic pollution control of dangerous substances (1976-2002).

512 Engasser, J.M., Horvath, C., 1976. Diffusion and kinetics with immobilized enzymes, Chapter in  
513 book: *Immobilized enzyme principles*. *Appl. Biochem. Bioeng.* edited by L.B. Wingard Jr, E.  
514 Katchalski-Katzir, L. Goldstein, New York, 1, 127-220.

515 EPA United States environmental protection agency Priority pollutant list, December 2014.

516 Frasconi, M., Favero, G., Boer, H., Koivula, A., Mazzei, F., 2010. Kinetic and biochemical properties  
517 of high and low redox potential laccases from fungal and plant origin. *Biochim. Biophys. Acta.* 1804,  
518 899–908. <https://doi.org/10.1016/j.bbapap.2009.12.018>

519 Gianfreda, L., Xu, F., Bollag, J.M., 1999. Laccase a useful group of oxidoreductive enzymes.  
520 *Bioremed. J.* 3, 1–25. <https://doi.org/10.1080/10889869991219163>

521 Gianfreda, L., Sannino, F., Rao, M.A., Bollag, J.M., 2003. Oxidative transformation of phenols in  
522 aqueous mixtures. *Water Res.* 37, 3205-15. [https://doi.org/10.1016/S0043-1354\(03\)00154-4](https://doi.org/10.1016/S0043-1354(03)00154-4)

523 Girelli, A.M., Mattei, E., Messina, A., 2007. Immobilized tyrosinase reactor for on-line HPLC  
524 application development and characterization. *Sensor. Actuat. B* 121, 515–  
525 521. <https://doi.org/10.1016/j.snb.2006.04.076>

526 Girelli, A.M., Quattrocchi, L., Scuto, F.R., 2020. Silica-chitosan hybrid support for laccase  
527 immobilization. *J. Biotechnol.* 318, 45-50. <https://doi.org/10.1016/j.jbiotec.2020.05.004>

528 Glazunova, A.O., Trushkin, N.A., Moiseenko, K.V., Filimonov, I.S., Fedorova, T.V., 2018. catalytic  
529 efficiency of basidiomycete laccases: redox potential versus substrate-binding pocket Structure.  
530 *Catalysts.* 8, 152. <https://doi.org/10.3390/catal8040152>.

531 Goldstein, L.G., 1976. Kinetic behaviour of immobilized enzyme systems methods. *Enzymol.* 44,  
532 397-443. [https://doi.org/10.1016/S0076-6879\(76\)44031-4](https://doi.org/10.1016/S0076-6879(76)44031-4)

533 Gonzalez, M.D., Vidal, T., Tzanov, T., 2009. Electrochemical study of phenolic compounds as  
534 enhancers in laccase-catalyzed oxidative reactions. *Electroanalysis.* 20, 2249–  
535 2257. <https://doi.org/10.1002/elan.200904678>

536 Guzik, U., Kocurek, K.H., Wojcieszynska, D., 2014. Immobilization as a strategy for improving  
537 enzyme properties-application to oxidoreductases. *Molecules* 19, 8995-  
538 9018. <https://doi.org/10.3390/molecules19078995>

539 Jankowska, K., Ciesielczyk, F., Bachosz, K., Zdarta, J., Kaczorek E., and Jesionowski, T., 2019.  
540 Laccase Immobilized onto Zirconia–Silica Hybrid Doped with Cu<sup>2+</sup> as an Effective Biocatalytic  
541 System for Decolorization of Dyes. *Materials*. 12, 1252. <https://doi.org/10.3390/ma12081252>

542 Ji, C., Nguyen, L.N., Hou, J., Hai, F.I., Chen, V., 2017. Direct immobilization of laccase on titania  
543 nanoparticles from crude enzyme extracts of *P.ostreatus* culture for micro-pollutant degradation. *Sep.*  
544 *Purif. Technol.* 178, 215–223. <https://doi.org/10.1016/j.seppur.2017.01.043>

545 Kasaai, M.R., 2009. Various methods for determination of the degree of N-acetylation of chitin and  
546 chitosan: A Review. *J. Agric. Food Chem.* 57 (2009) 1667–1676.

547 Kordatou, I.M., Karaolia, P., Fatta-Kassinos, D., 2017. The role of operating parameters and oxidative  
548 damage mechanisms of Advanced Chemical Oxidation Processes in the combat against antibiotic-  
549 resistant bacteria and resistance genes present in urban wastewater. *Water Res.* 129, 208-  
550 230 <https://doi.org/10.1016/j.watres.2017.10.007>

551 Kulkarni, S.J., Kaware, D.J.P., 2013. Review on research for removal of phenol from waste- water.  
552 *Int. J. Sci. Res. Public.* 3, 1–4.

553 Lamuela-Raventós, R.M., 2018. Folin–Ciocalteu method for the measurement of total phenolic  
554 content and antioxidant capacity, Chapter 6 in Book: *Measurement of Antioxidant Activity &*  
555 *Capacity: Recent Trends and Applications*, First Edition, Edited by R. Apak, E. Capanoglu Istanbul,  
556 F. Shahidi, 107-114. <https://doi.org/10.1002/9781119135388.ch6>

557 Liu, Y., Zeng, Z., Zeng, G., Tang, L., Pang, Y., Li, Z., Liu, C., Lei, X., Wu, M., Ren, P., Liu, Z.,  
558 Chen, M., Xie, G., 2012. Immobilization of laccase on magnetic bimodal mesoporous carbon and the  
559 application in the removal of phenolic compounds. *Biores. Technol.* 115, 21-  
560 26. <https://doi.org/10.1016/j.biortech.2011.11.015>

561 Mahat, N.A., Onoja, E., 2016. Relevant techniques and mechanisms for enzyme immobilization,  
562 Chapter 2 In book: *Protocols and methods for developing green immobilized nanobiocatalysts for*  
563 *esterification reactions*. Editors: R.A. Wahab, N.A. Mahat, 31-52.

564 Moldes-Diz, Y., Gamallo, M., Eibes, G., Vargas-Osorio, Z., Vazquez-Vazquez, C., Feijoo, G.,  
565 Lema, J. M., Moreira, M. T., 2018. Development of a superparamagnetic laccase nanobiocatalyst  
566 for the enzymatic biotransformation of xenobiotics. *J. Environ. Eng.*, 144, 04018007.

567 Mohammadi, M., As’habi, M.A., Salehi, P., Yousefi, M., Nazari, M., Brask, J., 2018. Immobilization  
568 of laccase on epoxy-functionalized silica and its application in biodegradation of phenolic  
569 compounds. *Int. J. Biol. Macromol.* 109, 443-447. <https://doi.org/10.1016/j.ijbiomac.2017.12.102>

570 Mulinacci, N., Romani, A., Galardi, C., Pinelli, P., Giaccherini, C., Vincieri, F.F.,  
571 2001. Polyphenolic content in olive oil waste waters and related olive samples. *J. Agric. Food Chem.*  
572 49, 3509-3514. <https://doi.org/10.1021/jf000972q>

573 Papadaki, M., Emery, R.J., Abu-Hassan, M.A., Diaz-Bustos, A., Metcalfe, I. S., Mantzavinos, D.  
574 2004 Sono catalytic oxidation processes for the removal of contaminants containing aromatic rings  
575 from aqueous effluents. *Sep. Purif. Technol.* 34, 35–42. [https://dx.doi.org/10.1016/S1383-](https://dx.doi.org/10.1016/S1383-4755866(03)00172-22)  
576 [475 5866\(03\)00172-22](https://dx.doi.org/10.1016/S1383-4755866(03)00172-22)

577 Pardo, I., Camarero, S., 2015. Laccase engineering by rational and evolutionary design. *Cell. Mol.*  
578 *Life Sci.* 72 , 897–910. <https://doi.org/10.1007/s00018-014-1824-8>

579 Rahmani, K., Ali, M., Amir, F., Mahvi, H., Gholami, M., Esrafil, A., Forootanfar, H. , Farzadkia,  
580 M., 2015. Elimination and detoxification of sulfathiazole and sulfamethoxazole assisted by laccase  
581 immobilized on porous silica beads. *Int. Biodeterior. Biodegrad.*, 97, 107-114.  
582 <https://doi.org/10.1016/j.ibiod.2014.10.018>

583 Rahmanian, N., Jafari, S.M., Galanakis, C.M., 2013. Recovery and removal of phenolic compounds  
584 from olive mill wastewater. *J. Am. Oil Chem. Soc.* 91, 1-18. [https://doi.org/10.1007/s11746-013-](https://doi.org/10.1007/s11746-013-2350-9)  
585 [2350-9.](https://doi.org/10.1007/s11746-013-2350-9)

586 Rayati, S, Nejabat, F., 2017. Catalytic activity of Fe-porphyrins grafted on multiwalled carbon  
587 nanotubes in the heterogeneous oxidation of sulfides and degradation of phenols in water. *C R Chim.*  
588 20, 967-974. [https://doi.org/10.1016/j.crci.2017.05.004.](https://doi.org/10.1016/j.crci.2017.05.004)

589 Re, R., Pellegrini, N., Proteggente, A., Pannala, A., Yang, M., Rice-Evans, C., 1999. Antioxidant  
590 activity applying an improved ABTS radical cation decolorization assay. *Free Radical Biol. Med.* 26,  
591 1231–1237. [https://doi.org/10.1016/S0891-5849\(98\)003153](https://doi.org/10.1016/S0891-5849(98)003153)

592 Rohindra, D.R., Nand, A. V, Khurma, J.R., 2004. Swelling properties of chitosan hydrogels. *South*  
593 *Pacific J. Nat. Appl. Sci.* 22, 32–35.

594 Scheiblbrandner, S., Breslmayr, E., Csarman, F., Paukner, R., Führer, J., Herzog, P. L., Shleev, S.V.,  
595 Osipov, E. M., Tikhonova, T. V., Popov, V.O., Haltrich, D., Ludwig, R., Kittl, R., 2017. Evolving  
596 stability and pH-dependent activity of the high redox potential *Botrytis aclada* laccase for enzymatic  
597 fuel cells. *Nature* 7,13688. <https://doi.org/10.1038/s41598-017-13734-0>

598 Soni, U., Bajpai, J., Singh, S.K., Bajpai, A.K., 2017. Evaluation of chitosan-carbon based  
599 biocomposite for efficient removal of phenols from aqueous solutions. *J. Water Process Eng.* 16., 56–  
600 63. [https://doi.org/10.1016/j.jwpe.2016.12.004.](https://doi.org/10.1016/j.jwpe.2016.12.004)

601 Stasinakis, A.S., 2008. Use of selected advanced oxidation processes (AOPs) for wastewater  
602 treatment – A mini review. *Global Nest J.* 10, 376-385. <https://doi.org/10.30955/gnj.000598>

603 Tavares, A. P.M., Rodríguez, O., Fernández-Fernández, M., Domínguez A., Moldes, D., Sanromán,  
604 M. A., Macedo, E. A., 2013. Immobilization of laccase on modified silica: Stabilization, thermal  
605 inactivation and kinetic behaviour in 1-ethyl-3-methylimidazolium ethylsulfate ionic liquid.  
606 *Biores. Technol.* 131, 405-412. <https://doi.org/10.1016/j.biortech.2012.12.139>

607 Tušek, A. J., Tišma, M., Bregović, V., Ptičar, A., Kurtanjek, Ž., Zelić, B., 2013. Enhancement of  
608 phenolic compounds oxidation using laccase from *Trametes versicolor* in a microreactor, *Biotechnol.*  
609 *Bioprocess. Eng.* 18, 686-696. <https://doi.org/10.1007/s12257-012-0688-8>

610 Villalobos, D.A., Buchanan, I.D., 2002. Removal of aqueous phenol by arthromyces ramosus  
611 peroxidase. *J. Environ. Eng. Sci.* 1, 65-73 <https://doi.org/10.1139/s01-003>

612 Villegas, L.G.C., Mashhadi, N., Chen, M., Mukherjee, D., Taylor, K.E., Biswas, N., 2016. A Short  
613 review of techniques for phenol removal from wastewater. *Curr. Pollution Rep.* 2, 157–  
614 167. <https://doi.org/10.1007/s40726-016-0035-3>.

615 Vione, D., Maurino, V., Minero, C., Pelizzetti, E., 2002. New processes in the environmental  
616 chemistry of nitrite: nitration of phenol upon nitrite photoinduced oxidation. *Environ. Sci. Technol.*  
617 36, 669-676. <https://doi.org/10.1021/es010101c>

618 Wang, Q.Z., Chen, X.G., Liu, N., Wang, S.X., Liu, C.S., Meng, X.H., Liu, C.G., 2006. Protonation  
619 constants of chitosan with different molecular weight and degree of deacetylation, *Carbohydrate*  
620 *Polymers.* 65, 194-201. <https://doi.org/10.1016/j.carbpol.2006.01.001>

621 Xu, F., Deussen, H.J., Lopez, B., Lam, L., Li, K., 2001. Enzymatic and electrochemical oxidation of  
622 N-hydroxy compounds, redox potential, electron transfer kinetics, and radical stability, *Eur. J.*  
623 *Biochem.* 268, 4169-4176. <https://doi.org/10.1046/j.1432-1327.2001.02328.x>.

624 Yu, Y., Hu, Z., Wang, Y., Gao, H., 2017. Magnetic SN-functionalized diatomite for effective  
625 removals of phenols. *Int. J. Miner. Process.* 162, 1–5. <https://doi.org/10.1016/j.minpro.2017.02.001>

626 Zhang, K., Yang, W., Liu, Y., Zhang, K., Chen, Y, Yin, X., 2020. Laccase immobilized on chitosan-  
627 coated Fe<sub>3</sub>O<sub>4</sub> nanoparticles as reusable biocatalyst for degradation of chlorophenol. *J. Mol.*  
628 *Struct.* 1220, 128769. <https://doi.org/10.1016/j.molstruc.2020.128769>

629 Zheng, F., Cui, B.K., Wu, X.J., Meng, G., Si, J., 2016. Immobilization of laccase onto chitosan beads  
630 to enhance its capability to degrade synthetic dyes. *Int. Biodeterior. Biodegrad.* 110, 69-  
631 78. <https://doi.org/10.1016/j.ibiod.2016.03.004>

632

633

634

635

636

637

638

639

640

641

642



643

644

645

646

**Table 1:** Elemental analysis of different types of chitosan, silica and composites (silica-CS)

	<b>Chitosan (CS1)</b>	<b>Chitosan (CS2)</b>	<b>Chitosan (CS3)</b>	<b>silica</b>	<b>silica- CS1</b>	<b>silica- CS2</b>	<b>silica- CS3</b>
<b>N%</b>	7.30	7.29	7.22	0	1.41	0.99	1.82
<b>C%</b>	40.14	40.63	40.71	0.13	7.02	5.67	10.47
<b>H%</b>	6.92	7.05	7.17	0.31	1.12	1.19	2.21
<b>C/N</b>	5.50	5.57	5.64	-	4.97	5.72	5.75

647

648

649

650

651

652

653

654

655

656

657

658

659

660

661

662

663

664

665  
666  
667  
668  
669  
670  
671  
  
672  
673  
674  
675  
676  
677  
678  
679  
680  
681  
682  
683  
684  
685  
686  
687  
688

**Table 2:** Effect of hydrodynamic parameters (flow rate) on apparent ( $K_m^{app}$  and  $V_{max}^{app}$ ) and inherent ( $K_m^{inh}$  and  $V_{max}^{inh}$ ) kinetic values and mass transport coefficient (h). Experimental conditions: IMER, pH 5, 30°C, substrate ABTS.

<b>flow rate</b> (mL/min)	<b><math>K_m^{app}</math></b> (mM)	<b><math>V_{max}^{app}</math></b> ( $\mu\text{mol}/\text{min}$ )	<b><math>K_m^{inh}</math></b> (mM)	<b><math>V_{max}^{inh}</math></b> ( $\mu\text{mol}/\text{sec} \cdot \text{m}^2$ )	<b>“h”</b> (cm/sec)
0.5	23.90	0.147	2.04	$5.5 \cdot 10^{-6}$	$5.63 \cdot 10^{-3}$
0.6	1.68	0.018	0.13	$1.1 \cdot 10^{-5}$	$0.98 \cdot 10^{-2}$
0.7	0.43	0.010	$0.65 \cdot 10^{-2}$	$2.8 \cdot 10^{-5}$	$1.74 \cdot 10^{-2}$
0.8	0.45	0.009	$0.62 \cdot 10^{-2}$	$3 \cdot 10^{-5}$	$1.53 \cdot 10^{-2}$

689  
690

**Table 3:** Operational and storage stability of laccase immobilized on various supports, recently published in literature, compared with those of the proposed biocatalyst

<b>Support</b>	<b>Application mode</b>	<b>Storage stability (residual activity)</b>	<b>Operational stability (residual activity)</b>	<b>Reference</b>
Chitosan@Fe <sub>3</sub> O <sub>4</sub>	batch	4 weeks 75.2%	10 cycles 72%	Zang et al., 2020
Zirconia silica hybrid support doped with Cu <sup>2+</sup>	batch	20 days 80%	7 cycles 40%	Jankowska et al.2019
Epoxy-funtionalized silica	batch	-	5 cycles 61%	Mohamadi et al. 2018
Silica@Fe <sub>3</sub> O <sub>4</sub>	batch	22 days 80%	8 cycles 70%	Moldes-Diz, 2018
Silica activated with glutaraldehyde	batch	7 days 70%	10 cycles 70%	Tavares et al. 2013
Silica-Ca-chitosan	continuous	70 days 70%	4 cycles and 105 injections 50%	Present study

691  
692  
693  
694  
695  
696  
697  
698  
699  
700  
701  
702  
703  
704  
705  
706  
707  
708

709

710

711 **Table 4:** Apparent and inherent kinetic parameters (  $K_m^{app}$ ,  $V_{max}^{app}$ ,  $K_m^{inh}$ ,  $V_{max}^{inh}$  ), transport  
 712 coefficient (h) of various phenols. Experimental conditions: IMER, pH 5, 30°C, substrate phenols,  
 713 flow rate 0.7 mL/min.

714

Phenol	$K_m^{app}$ (mM)	$V_{max}^{app}$ (peak area/min)	$K_m^{inh}$ (mM)	$V_{max}^{inh}$ (peak area/ s <sup>-1</sup> *m <sup>2</sup> )	h (10 <sup>-1</sup> cm peak area s <sup>-1</sup> mmol)
Caffeic acid	1.41	4587	2.59	3.53	2.99
Cathecol	8.05	1718	1.42	1.16	0.157
p-Coumaric acid	-	-	-	-	-
4-Methylcatechol	5.39	1976	1.05	1.62	0.184
Siringic acid	0.74	2074	1.32	2.06	1.27
Tyrosol	-	-	-	-	-
Vanillic acid	1.75	13624	1.11	1.48	0.052

715

716

717

718

719

720

721

722

723

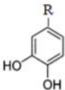
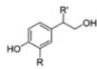
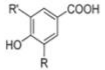
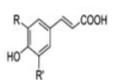
724

725

726

727

728 **Table 5:** Structural and chemical characteristics (pKa, octanol-water partition coefficient (logP),  
 729 redox potential) of phenols

Class	Structure	Compound	Functional groups	pKa <sup>a</sup>	LogP <sup>a</sup>	Redox potential*
Simple phenols		Catechol	R= H	9.45	0.88	+0.53 Canfora et al.2008
		4-Methyl catechol	R=CH <sub>3</sub>	-	1.37	-
Phenyl alcohols		Tyrosol	R=H R'=H	10.2	0.85	-
Hydroxy-benzoic phenols		Vanillic acid	R = OCH <sub>3</sub> R' = H	4.16	1.43	+0.71 Canfora et al.2008
		Syringic acid	R =OCH <sub>3</sub> R'= OCH <sub>3</sub>	3.93	1.04	+0.68 Gonzalez et al. 2009
Hydroxy-cinnamic phenols		p-Coumaric acid	R = H R' = H	4	1.74	+0.70 Gonzalez et al. 2009
		Caffeic acid	R = OH R' = H	3.14	1.53	+0.53 Canfora et al.2008

a: [https://chemaxon.com/products/calculators-and-predictors#logp\\_logd](https://chemaxon.com/products/calculators-and-predictors#logp_logd)

\*oxidation potential versus Ag/AgCl references electrode

730

731

732

733

734

735

736

737

738

739

740

741

742

743

744

745  
746  
747  
748  
749  
750  
752  
753  
754  
755  
756  
757  
758  
759  
760  
761  
762  
763  
764  
765  
766  
767  
768  
769  
770  
771  
772  
773

**Table 6:** Effect of total phenol amount on removal % from water. Experimental conditions: IMER, reaction time 8 and 14 h, pH 5, 30°C, continuous mode.

<b>Total phenols (mg/L)</b>	<b>% Removal (8 h)</b>	<b>% Removal (14 h)</b>
175	15	43
350	38	50
525	33	49

774 **Legends**

775 **Figure 1:** Scheme of oxidized laccase immobilized procedure

776 **Figure 2:** Thermal gravimetric curves pure silica (A), silica-chitosan medium molecular weight (B),  
777 silica-chitosan low molecular weight (C), silica-chitosan from shrimp shells (D) and pure chitosan  
778 (E). Experimental conditions: 1 mg of each samples, oxygen atmosphere, temperature range from 30  
779 to 700°C, and a scanning rate of 10 °C/min.

780 **Figure 3:** Reuse comparison between immobilized laccase on silica-CS1 (black histogram); silica-  
781 CS2 (dark gray) and silica-CS3 (grey) for 9 consecutive cycles in batch mode. Reaction conditions:  
782 30°C, pH 3 0.1 M citrate-0.2 M phosphate buffer, 0.18 mM 2,2-azinobis (3-ethylbenzothiazoline-6-  
783 sulfonate) as substrate. Values represent the mean  $\pm$  standard deviations (n=3). The first activity  
784 measured was set to 100%.

785 **Figure 4:** Recycle device used for dephenolization

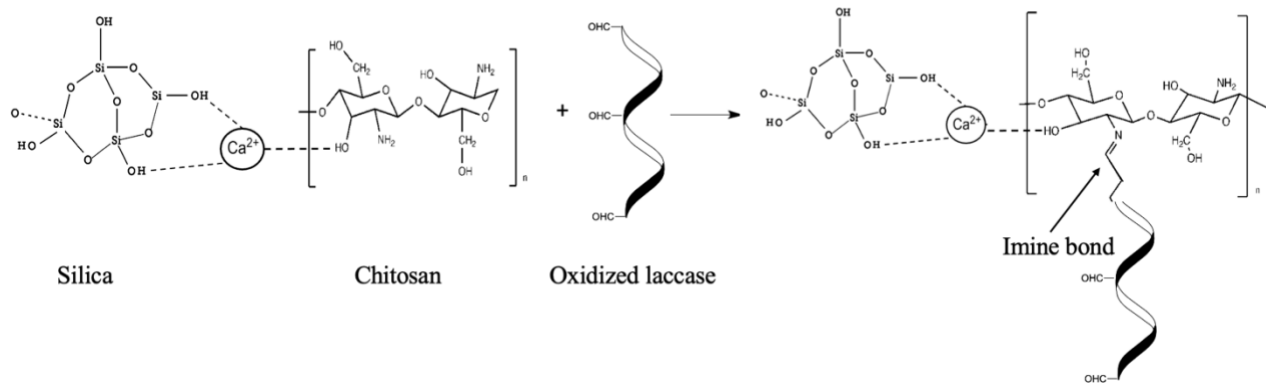
786 **Figure 5:** Storage stability (A) of free laccase (grey histogram) and IMER (black histogram) and  
787 operational stability (B) of IMER. Determination of laccase activity: i) free form: batch mode, 30°C,  
788 pH 3 and 0.2 mM 2,2-azinobis(3-ethylbenzothiazoline-6-sulfonate); ii) IMER (laccase immobilized  
789 on silica-CS1): continuous mode, 30°C, pH 5, injection volume 20  $\mu$ L 2.5 mM of 2,2-azinobis(3-  
790 ethylbenzothiazoline-6-sulfonate). IMER when not in use was stored at 4°C.

791  
792 **Figure 6:** Chromatographic profiles of the phenol mixture removal from water at three different  
793 times initial, 14 h and 21 h. Chromatographic conditions: stationary phase C18, mobile phase gradient  
794 elution: Pump A (MeOH: H<sub>2</sub>O with 1.3% HCOOH) and pump B (H<sub>2</sub>O): 0-24 min 15% pump A, 24  
795 to 35 min 50%, 35 to 38 min 50% and 38 to 40 min 20% A.

796  
797 **Figure 7:** Time-course degradation of phenol mixture by laccase immobilized on silica-CS1.  
798 Experimental conditions: continuous mode, flow rate 0.7 mL/min, 30°, pH 5, phenol concentration  
799 75 mg/mL

800  
801  
802  
803  
804  
805  
806  
807  
808  
809  
810  
811  
812  
813  
814  
815  
816  
817  
818  
819  
820

821  
822  
823  
824  
825  
826



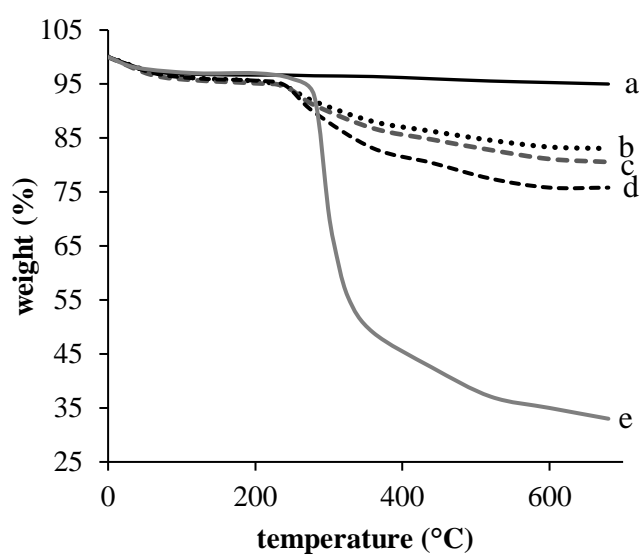
827  
828

829 Figure 1

830  
831  
832  
833  
834  
835  
836  
837  
838  
839  
840  
841  
842  
843  
844  
845

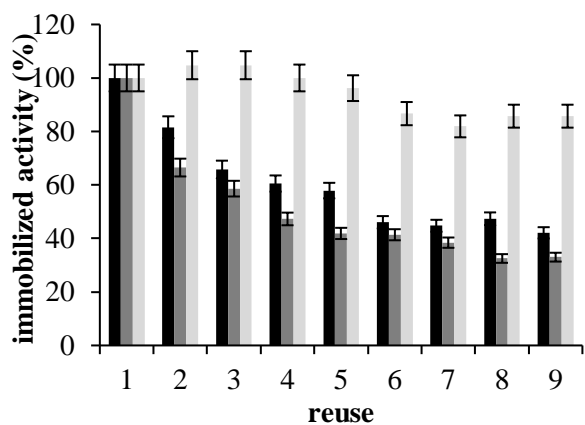


846  
847  
848  
849  
850  
851  
852  
853



854  
855  
856  
857  
858  
859  
860  
861  
862  
863  
864  
865  
866

**Figure 2**



867

868

869

870

871

872 **Figure 3**

873

874

875

876

877

878

879

880

881

882

883

884

885

886

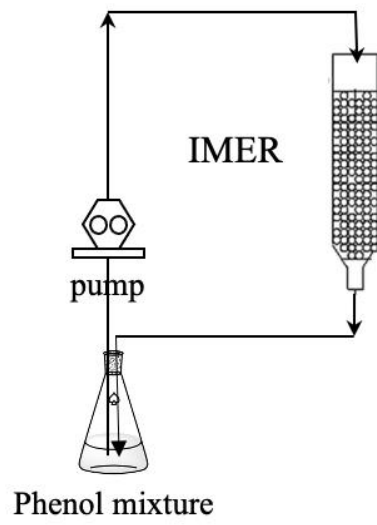
887

888

889

890

891



892

893

894

895

896

897 Figure 4

898

899

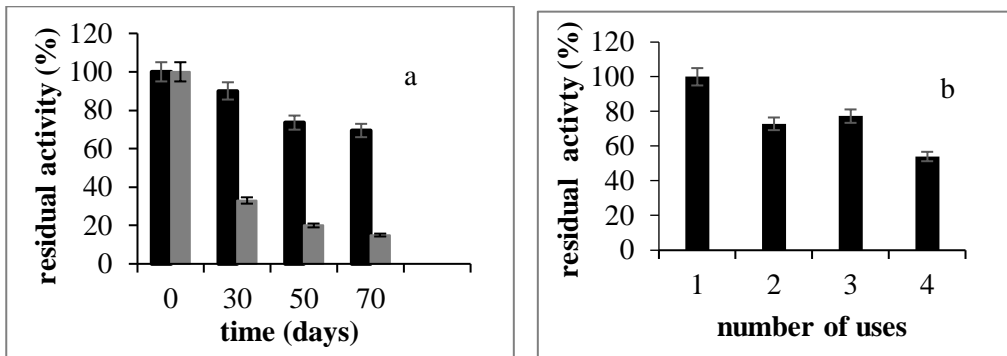
900

901

902

903

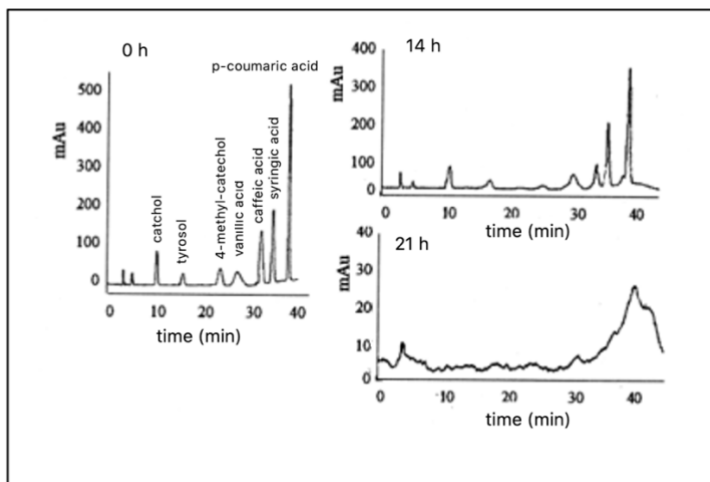
904  
905  
906  
907  
908  
909  
910



911  
912  
913  
914  
915  
916  
917  
918  
919  
920  
921  
922  
923  
924  
925  
926  
927

**Figure 5**

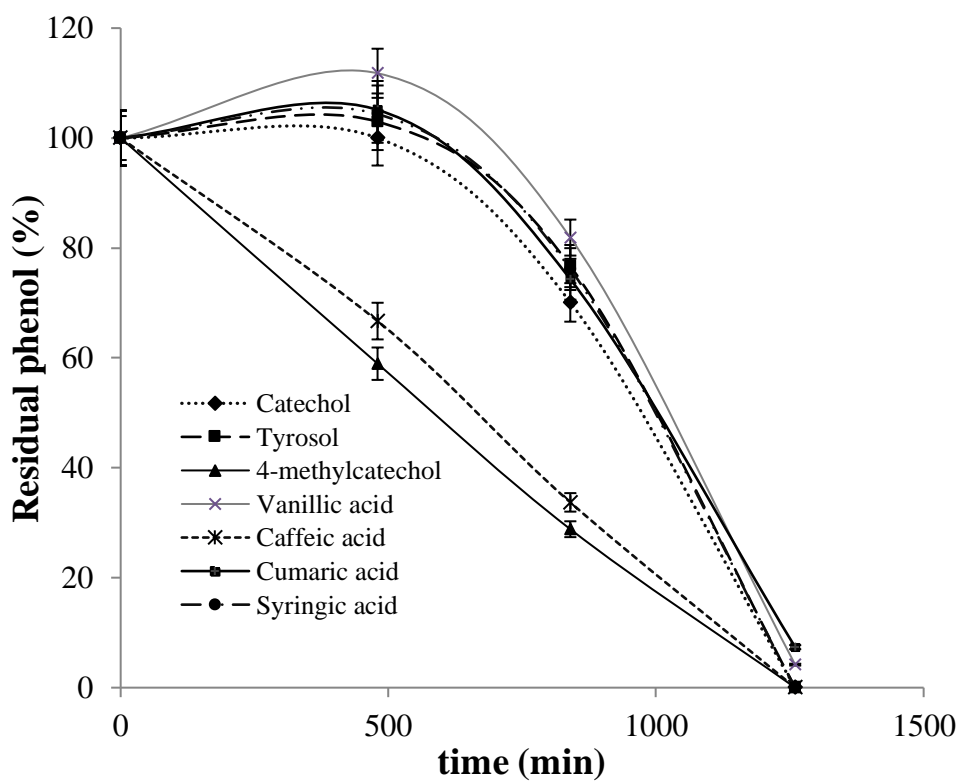
928  
929  
930  
931  
932  
933  
934



935  
936  
937  
938  
939  
940  
941  
942  
943  
944  
945  
946  
947  
948  
949

**Figure 6**

950  
951  
952  
953  
954  
955



956  
957  
958  
959

**Figure 7**

960  
961  
962  
963  
964  
965  
966  
967  
968  
969